Surface roughness, bulk, and reflectance characterization of SiC and Aluminum samples with PECVD-SiC cladding

*Issued by **R. Canestrari** and **D. Spiga** (INAF/OAB, Merate)*

*Reviewed by **G. Pareschi** and **M. Ghigo** (INAF/OAB, Merate)*

*SEM measurements performed by **C. Guaita** and **P. Fabbri** (RHODIA ITALIA, Ceriano Laghetto)*

*PROMAP measurements performed by **G. Destefanis** (MEDIA-LARIO TECHN., Bosisio Parini)*

*Reflectance measurements in visible-NIR light performed by **G. Toso** (INAF/OAB, Merate)*

*Reflectance measurements in Vacuum UV light performed by **P. Nicolosi** (LUXOR-INFM, Padova)*

*X-ray powder diffraction and Cathodoluminescence tests performed by **C. Ferrari, S. Arumainathan, G. Salviati** (IMEM-CNR, Parma)*

Istituto Nazionale di Astrofisica (INAF)
Via del Parco Mellini, 00100 Roma, Italy
Osservatorio Astronomico di Brera (OAB)
Via Brera 28, 20121 Milano, Italy
Via E. Bianchi 46, 23807 Merate, Italy

Table of Contents

Applicable Documents

[AD1] *Produzione di ottiche in SiC con processo "Plasma Enhanced Chemical Vapour Deposition"*, 2 Progress report, INAF/OAB – Galileo Avionica/CETEV Lab Proposal nel contesto MEF/INAF-UIT "PRISMA"

Reference documents

[RD1] Canestrari, R. , Valtolina, R. , Spiga, D. , Pareschi, G. *Characterization of a PECVD-SiC replicated mirror sample,* INAF/OAB Internal report 04/06

[RD2] J. B. Kortright and D. L. Windt, *Amorphous silicon carbide coatings for extreme ultraviolet optics*, Appl. Opt. 27, 2841 (1988)

Acronyms

CETEV CEntro TEcnologie del Vuoto (*Vacuum Technologies Center*)
CL CathodoLuminescence
INAF Istituto Nazionale di Astrofisica (*National Institute for Astrophysics*)
INFM Istituto Nazionale di Fisica della Materia (*National Institute for Physics of Matter*)
NIR Near InfraRed
OAB Osservatorio Astronomico di Brera (*Brera Astronomical Observatory*)
PECVD Plasma-Enhanced Chemical Vapour Deposition
PSD Power Spectral Density
VUV Vacuum UltraViolet
XRD X-Ray Diffraction
XRR X-Ray Reflectivity
XRS X-Ray Scattering

1. Introduction

The aim of this document is the presentation of the topographic and X-Ray (XRR, XRS and XRD) characterization of *Silicon Carbide* samples, deposited by PECVD onto substrates of two different types: a) substrates in SiC and b) substrates in Al. The samples are circular, with 1 inch diameter. All samples have been produced by Galileo Avionica CETEV. The samples are named hereafter as a) SiC-SiC and b) SiC-Al.

The present characterization is performed in the framework of the ***INAF/OAB and Galileo Avionica/CETEV Lab study*** **for the project MEF/INAF-UIT "PRISMA", WP 4200 and 4300** [AD1].

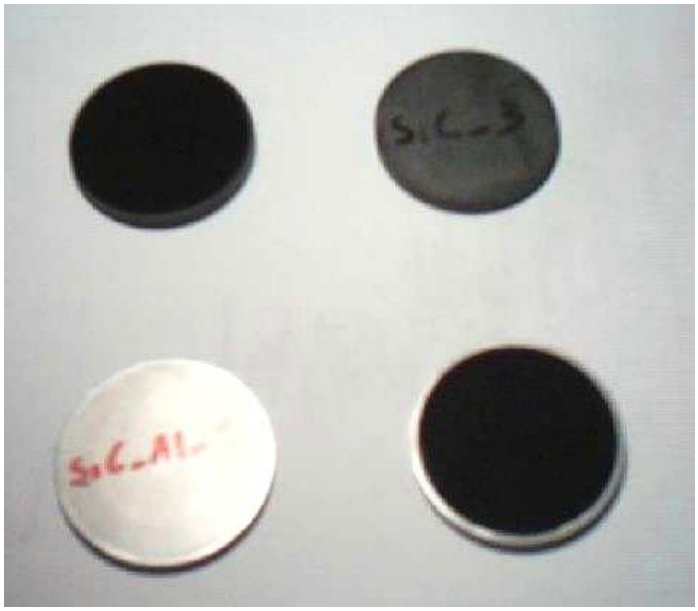

Fig.1:The samples being characterized in the present document.(top) two samples with Silicon Carbide substrates,(bottom) two samples with substrates in Aluminum. The SiC claddings have been deposited with the PECVD technique.

2. Surface topography characterization

2.1 Nomarski microscope

As a first investigation of the SiC surface, we inspected the samples by means of a *phase contrast Nomarski microscope* (see Fig. 2). This instrument cannot return a quantitative surface mapping.

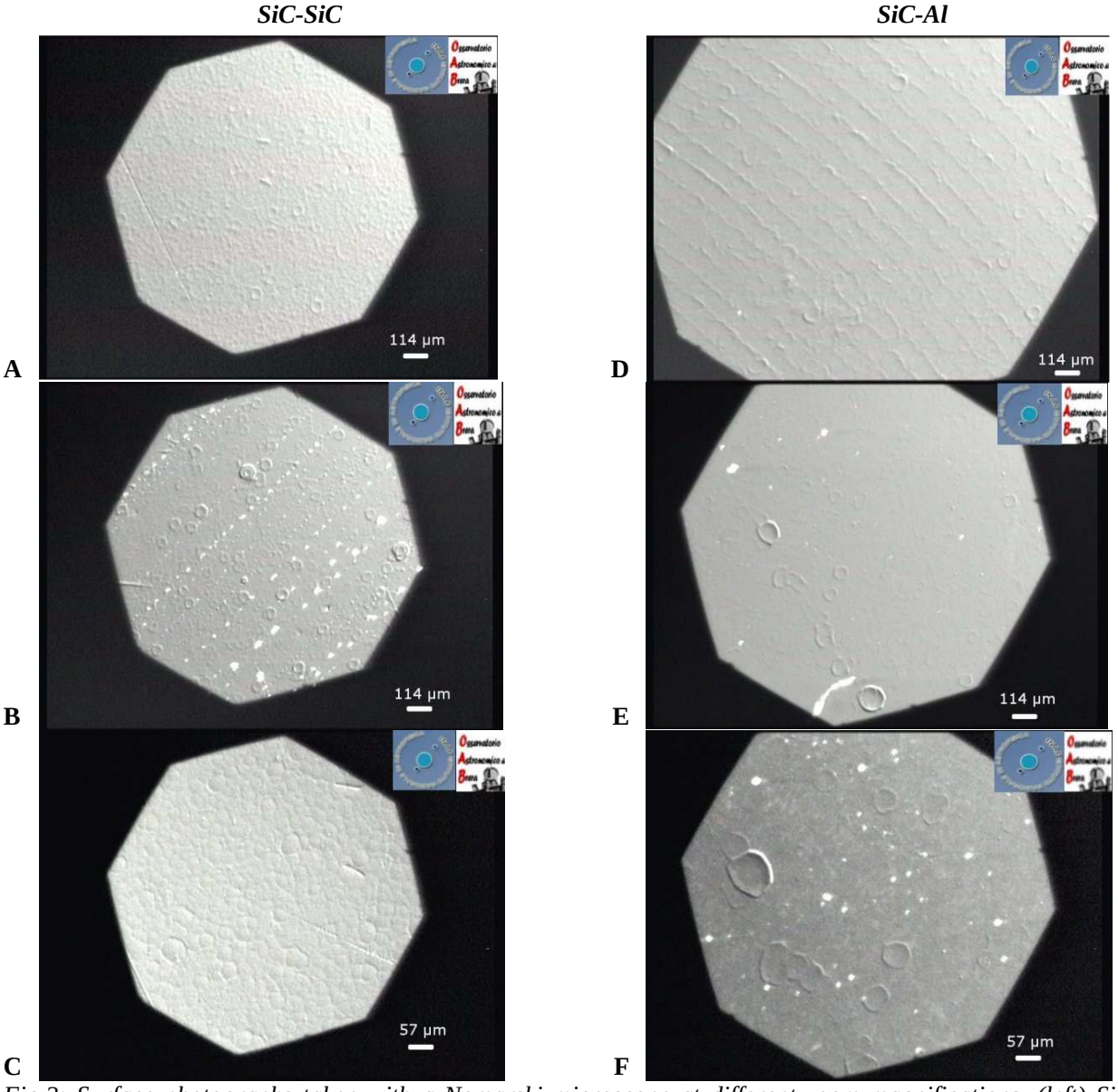

Fig.2: Surface photographs taken with a Nomarski microscope at different zoom magnifications. (left) SiC-SiC samples; (right) SiC-Al samples. A diffuse honeycomb structure is visible (C). Surface undulations also appear superimposed to the hexagonal texture (D)

One can readily see from the photos C and F in Fig. 2 that the surface of all samples is completely covered by an hexagonal texture. This structure is more uniform in the SiC-SiC samples. The typical size of the hexagons is about 50 μm. The honeycomb structure could either be inherited from a polycrystalline texture of the SiC cladding, or, in case of growth with amorphous structure, it could be a feature related to the deposition/polishing process. Some points (D) exhibit a preferential direction of surface features.

2.2 WYKO® profilometer

The surface microroughness was quantitatively measured by means of the optical profilometer WYKO®. Roughness measurements were carried out with both instrument heads (2,5x and 20x magnifications) available at INAF/OAB to cover a spatial frequencies range from 5 mm down to a few tenth microns.

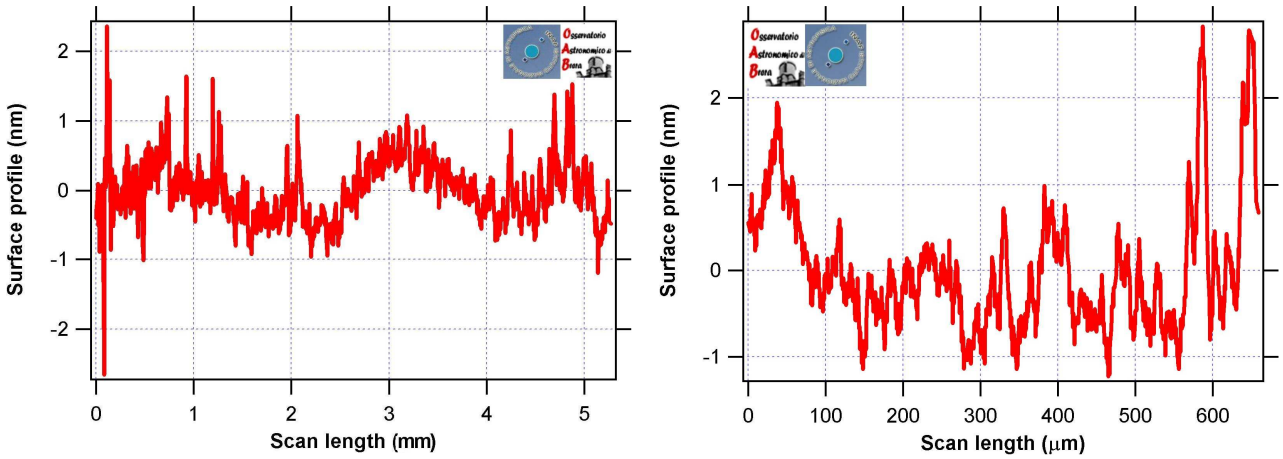

Fig.3: Two SiC-SiC samples surface profiles as measured with the optical profilometer WYKO. (left) ***2.5x*** *magnification:* ***σ = 14 Å*** *- (right)* ***20x*** *magnification:* ***σ = 4.6 Å***

To average out local features of the topography and to minimize the statistical error we sampled the surface in 5 different points for each sample. The roughness PSD of each sample has been computed by averaging the PSD of the 5 profiles. We present in Fig. 3 some profiles and the average PSD for the SiC-SiC samples. Some profiles of the SiC-Al samples are reported in Fig. 4, with the PSD averaged over the samples set.

The PSD computed with WYKO at the to magnification is consistent for the SiC-Al samples. For the SiC-SiC the two PSD do not overlap (Fig. 5), probably due to selection effects in the 20x measurement.

In the spatial frequency window of WYKO profiles a PSD comparison between the two types of samples can be carried out (Fig. 5). The two PSDs differ in the region [200÷30] μm, as the SiC-SiC samples exhibit a PSD bump at these spatial wavelengths. This spectral region corresponds to the scale size of the hexagons being seen in the Nomarski images (Fig. 2), and more apparent in the SiC-SiC surface photos.

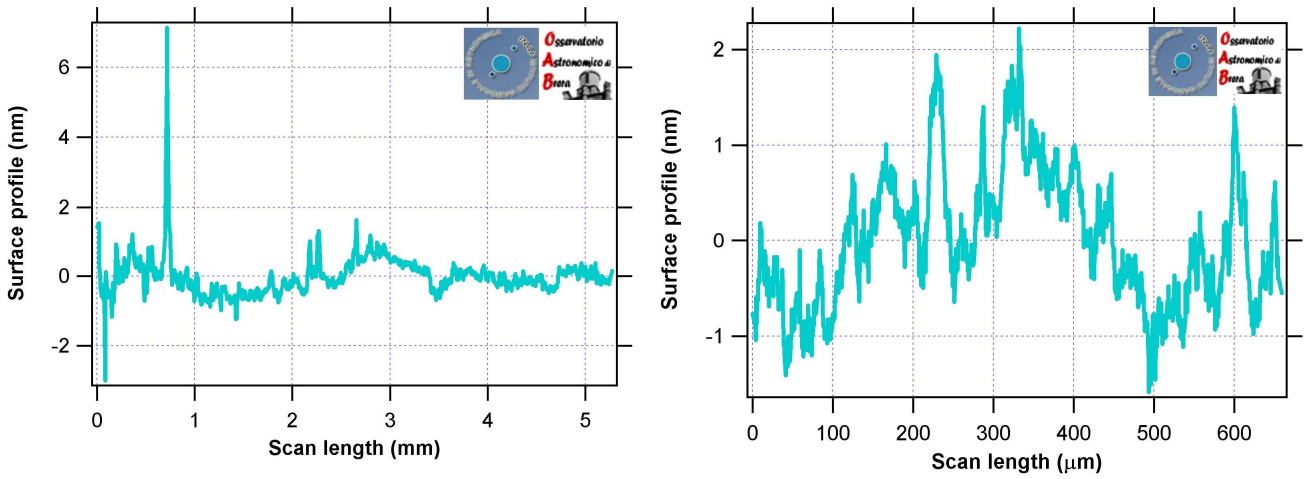

Fig.4: Two SiC-Al samples surface profiles as measured with the optical profilometer WYKO. (left) 2.5x magnification: ***σ = 5.8 Å*** *- (right) 20x magnification:* ***σ =5.4 Å***

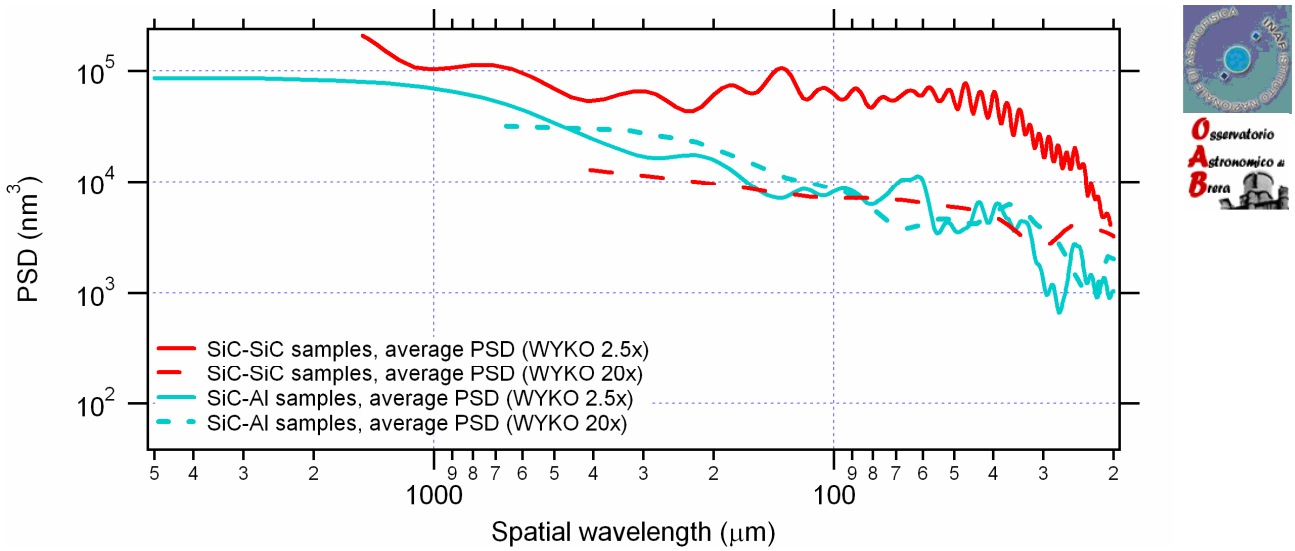

Fig. 5: Comparison between the PSDs of SiC-SiC samples (red line) and SiC-Al samples (blue lines). The bump around 50 μm could be due to the honeycomb texture, which is more clearly seen on the SiC-SiC samples surfaces.

2.3 PROMAP® measurements

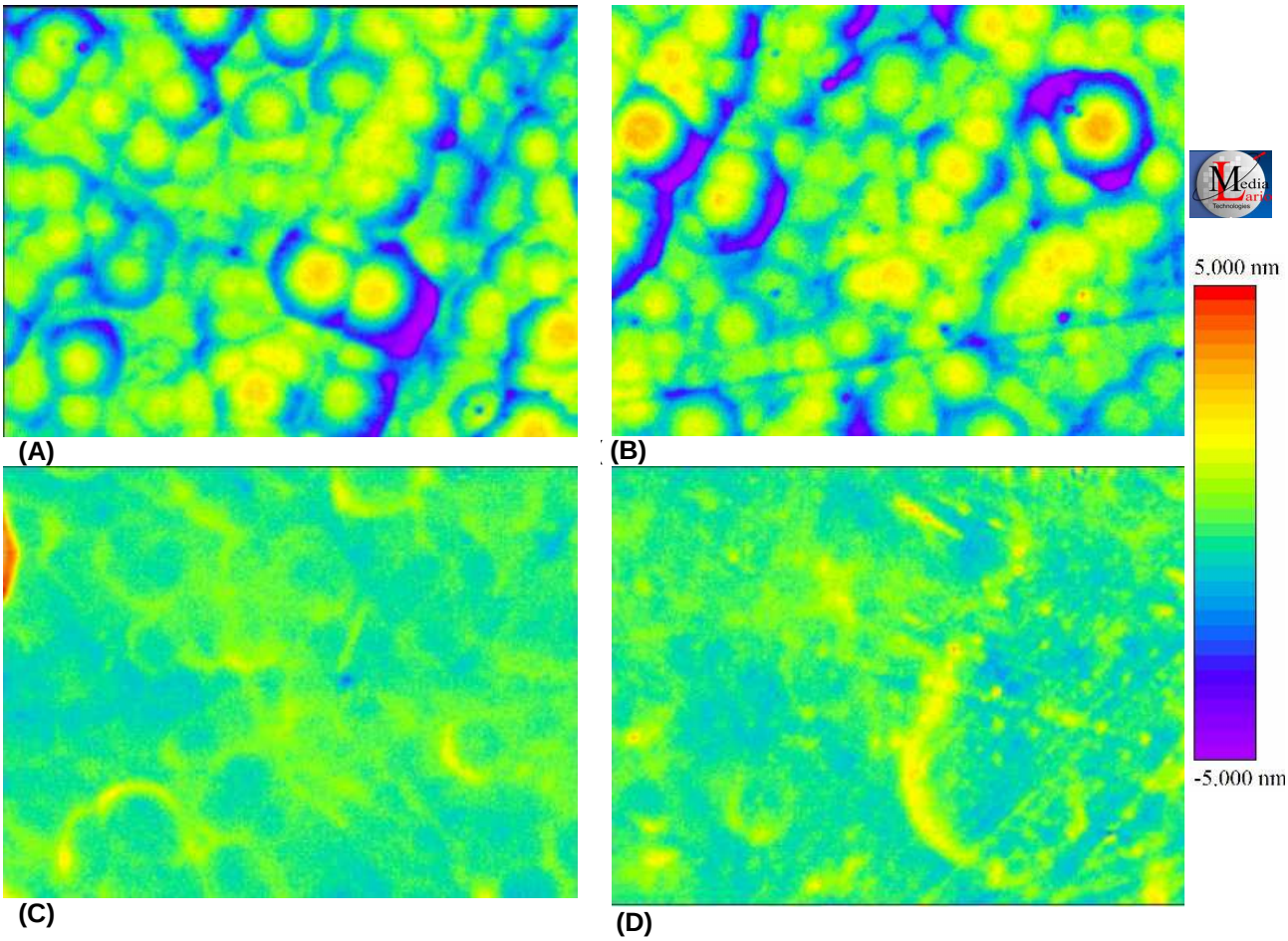

Fig. 6: some images of the samples surfaces obtained with PROMAP (courtesy of Media-Lario techn., *Bosisio Parini, Italy).* ***(A-B): SiC-SiC samples, σ ≈ 9.5 Å. (C-D): SiC-Al samples σ ≈ 5.5 Å****. The images size is* ***157x118 µm****. The vertical scale is reported on the right.*

PROMAP® images of the samples surface (see Fig. 6) were also taken at *Media-Lario techn.*, returning a 2D mapping of some sampled topography of the surface. The landscape of the SiC-SiC samples (Fig 6, A-B) appears at first glance rougher than the SiC-Al ones (Fig 6, C-D). Concerning the rms roughness, it is twice as large for SiC-SiC samples (9.5 Å vs. 5.5 Å for SiC-Al samples) in a spectral range 157 ÷ 3 µm. The different aspect of the two samples is evident also from WYKO measurements and from the visual inspection with the Nomarski microscope (see Sect. 2.1 and 2.2).

3. X-Ray (8.05 keV) samples characterization at INAF/OAB

The X-ray tests have been performed by means of a BEDE-D1 triple-axis diffractometer, with a Cu-anode X-ray tube as X-ray source. The Cu-Kα X-ray line (8.05 keV) has been filtered using a Si CCC monochromator. We could thereby probe the surface with a thin (70 μm wide) and collimated (20 arcsec divergent) X-ray beam; this setup has been maintained for all the X-ray measurements being reported.

3.1 X-Ray Reflectivity (XRR) measurements

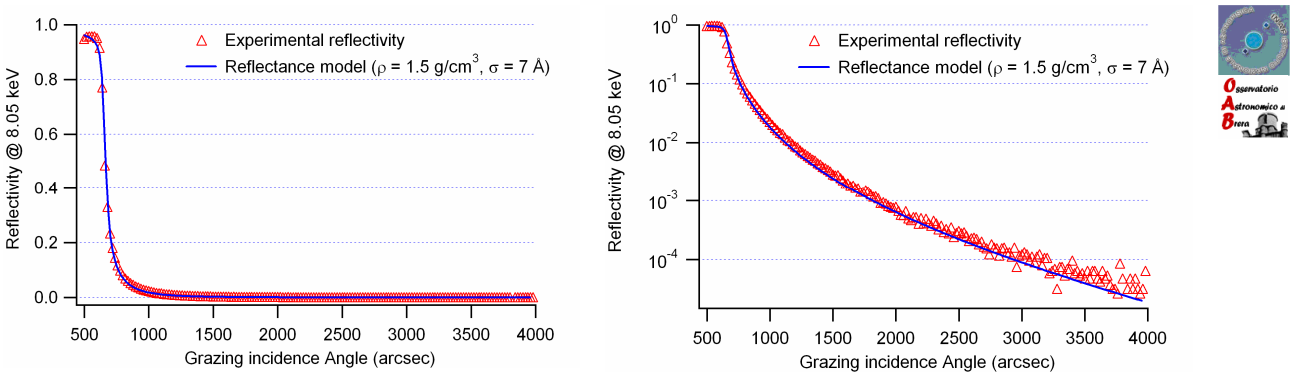

Fig. 7: an XRR scan of a SiC-SiC sample at 8.05 keV (left) linear scale - (right) log scale. The experimental data are well fitted by a model (computed with the IMD package) assuming a density much lower than the natural one (1.5 vs. 3.21 g/cm³) and a roughness rms of 7 Å

The XRR measurement consists in probing the reflectance of X-rays at a fixed energy, for different incidence angles. An XRR scan (at 8.05 keV) is plotted in Fig. 7: experimental data are well superimposed to a reflectivity model. The XRR curve exhibits a cut-off angle at 700 arcsec, related to the material density and to the photon energy in use (and, in a lesser extent, to the chemical composition). Surface microroughness also affects the reflectivity, especially at large incidence angles.

From the XRR fit we can infer a SiC cladding ***density ρ= 1.5 g/cm³*** and a surface ***roughness rms σ= 7 Å.*** This rms value should be referred to the spatial wavelengths smaller than ~15 μm. It is thereby fully consistent with the XRS data being reported in the next Sect.ion (see also Tab.1). Moreover, the density is only 50 % of the density value for the bulk (crystalline) density of SiC (3.2 g/cm³), that could mean an amorphous structure of the material (see also Sect. 3.3).

Finally, no interference features are visible: this means that at such incidence angles all the X-ray beam is absorbed in the SiC cladding and only the outer surface is probed in XRR and XRS measurements (see Sect. 3.2).

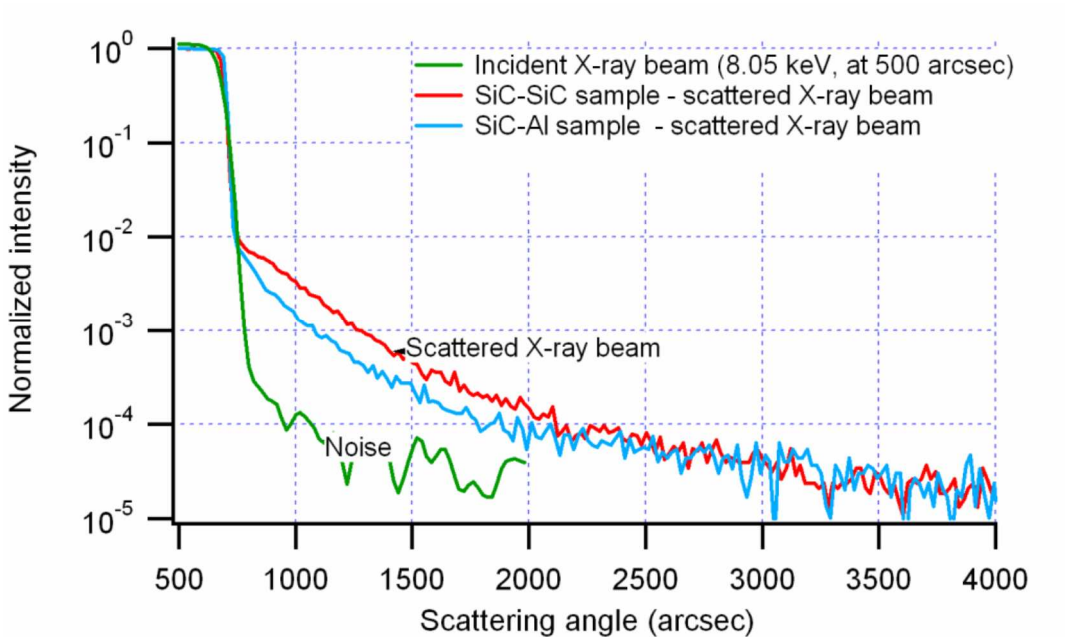

Fig. 8:normalized XRS diagrams (blue and red lines) for the SiC-SiC and SiC-Al samples at 8.05 keV. The scattered radiation is clearly visible when compared to a scan of the incident X-ray beam.

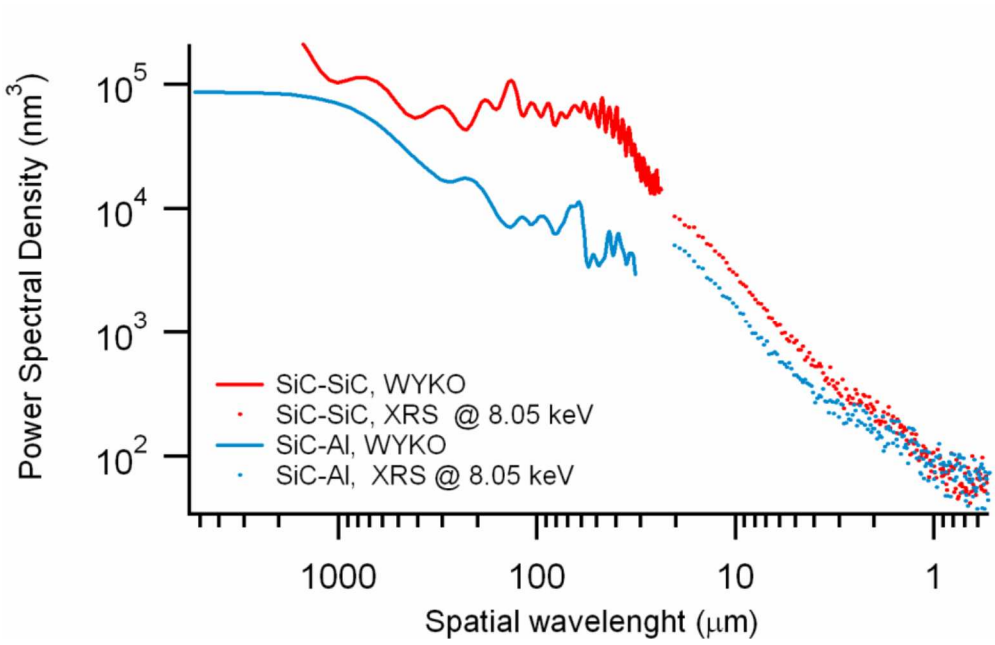

Fig. 9:the average surface PSD of the SiC-SiC samples and that of the SiC-Al samples, as measured with XRS (dots). The results are consistent with WYKO data (lines). The roughness σ in the XRS spectral band are ***8.7 Å for the SiC-SiC and 7 Å for the SiC-Al****.*

3.2 X-Ray Scattering (XRS) measurements

The surface PSD of the samples under test has also been measured directly from the X-ray scattering at 8.05 keV. The incidence angle was fixed at 500 arcsec (in the total external reflection regime) and the distribution of scattered photons at higher angles than the specular one was measured as a function of the scattering angle (see Fig. 8). The scattering intensity enables the calculation of the surface PSD, averaged over all the sampled surface (a few cm²). The computed PSDs cover a spatial wavelengths range between 20 and 0.6 μm (see Fig. 9).

The PSD as computed from the XRS diagrams is quite consistent with the WYKO data, even if the spectral ranges do not overlap. It is readily seen that the SiC-SiC samples scatter X-rays more than SiC-Al samples (Fig.8). This is also made apparent by the roughness rms of the samples (**8.7 Å for SiC-SiC** and **7 Å for SiC-Al**, see also Tab.1).

In Tab. 1 we summarize the results obtained with the different techniques.

Tab.1: Results overview for surface microroughness measurements..

Technique	***Spatial wavelength range [μm]***	σ_{RMS} ***[Å]***	
		SiC-SiC	***SiC-Al***
WYKO 2.5x	*[2000 ÷ 25]*	*14.0*	*5.8*
WYKO 20x	*[660 ÷ 25]*	*4.6*	*5.4*
PROMAP	*[150 ÷ 1]*	*9.5*	*5.5*
XRS @ 8.05 keV	*[20 ÷ 0.6]*	*8.7*	*7*
XRR	$[\sim 15 \div 7 \times 10^{-5}]$	*7*	*7*

3.3 X-Ray Diffraction (XRD) measurements at INAF/OAB and CNR-IMEM

The crystalline microstructure has also been probed by means of the X-ray Diffraction (XRD). A possible measurement (with a non-imaging detector) consists in a large-angle (>10 deg) X-ray reflectance scan with an intense X-ray beam (more than 300000 ph/sec) impinging on the sample. At such angles, the surface reflectivity is negligible. However, in presence of ***randomly-oriented*** crystallites, sharp diffraction peaks would be observed at incidence angles θ_i satisfying the ***Bragg law***

$$2D_{hkl} \sin \vartheta_i = \lambda$$

where λ is the X-ray wavelength in use and D_{hkl} is the distance between crystalline planes determined by the crystalline structure and the planes orientation, with respect to the incidence plane, specified by the Miller indices <*hkl*>. Assuming a crystallization in the hexagonal system (the most stable for SiC), the d-spacings D_{hkl} would generate XRD peaks at least at the following angles, corresponding to different diffracting planes in the crystals: 19.05 deg <101>, 16.77 deg <100>, 17.80 deg <201>, 30.02 deg <110>, 32.86 deg <103>, 36.02 deg <112>, as measured from the surface, with decreasing intensity.

Fig. 10 reports a large angular scan in the [3÷45] deg range for a SiC-Al sample. Several diffraction peaks were detected. Only one of these (at 19.05 deg) is in a theoretically-predicted positions for SiC, but the others are absent: this could be explained only by assuming the planes <101> of the SiC to be aligned to the sample surface.

Conversely, the XRD peak positions match very well the d-spacings of Aluminum (being utilized as sample substrate), at 19.05 deg <111>, 22.14 deg <200>, 39.01 deg <311>. Then, the diffraction peaks being observed are likely due to the polycrystalline structure of the Al substrate. Weaker peaks are also detected (likely due to hydrated Al oxide), and an intense peak beyond 40 deg, corresponding to Fe or Cr d-spacings that can contaminate the Aluminum substrate.

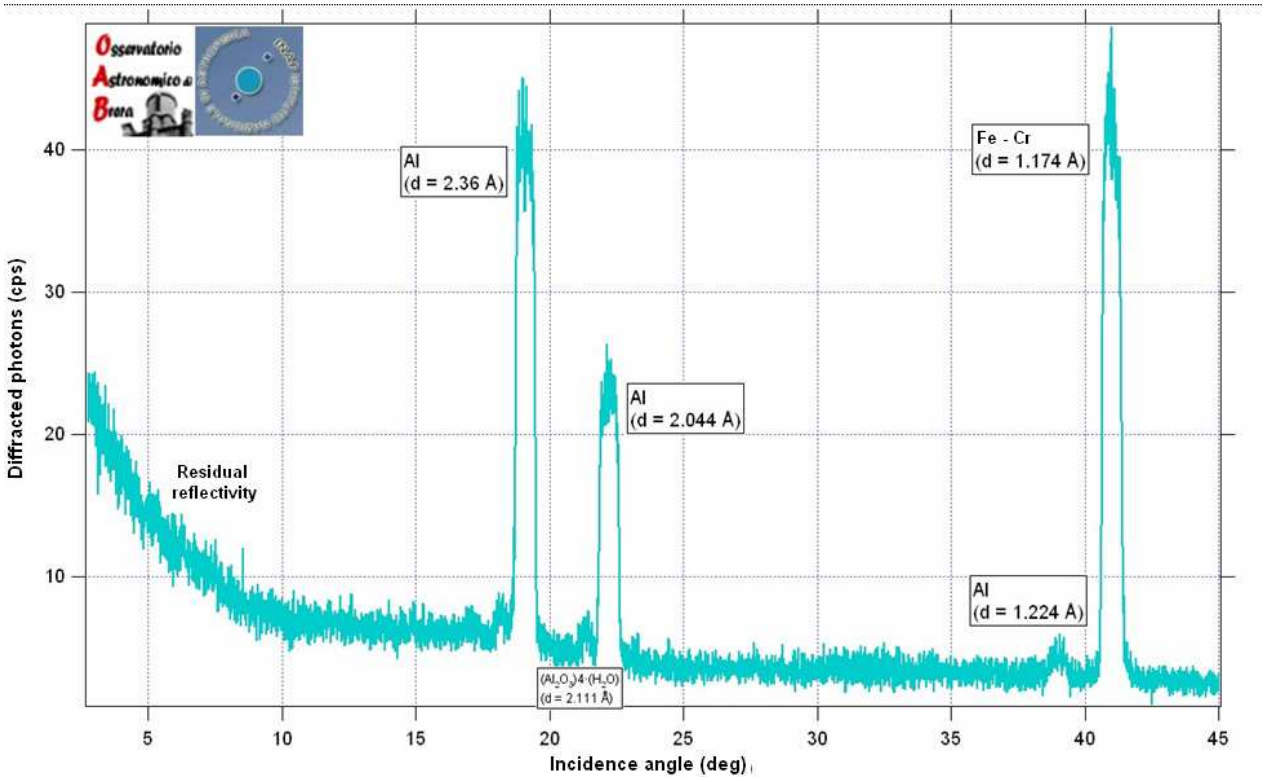

Fig. 10: an XRD scan of a SiC-Al sample (performed at INAF/OAB). The observed peak positions do not match a Silicon Carbide crystalline structure.

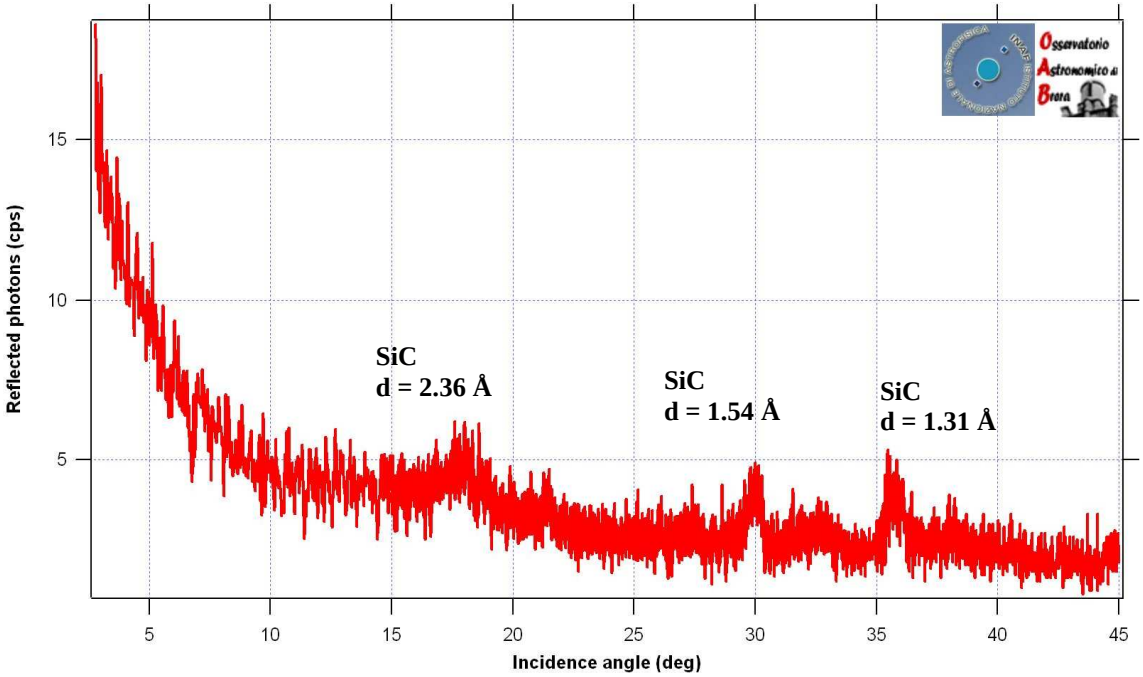

Fig. 11: an XRD scan of a SiC-SiC sample (performed at INAF/OAB). The small XRD peaks match the d-spacings of SiC and could be due to a polycrystalline structure of the SiC substrate.

Concerning the XRD scans of the SiC-SiC samples (Fig. 11), only small peaks appear (at 19.05 - 30.02 – 36.02 deg). They correspond to the d-spacing of SiC for 3 selected orientations of the crystals. Their absolute absence in the XRD scan of Fig. 10, however, probably indicates that they could be related to a *polycrystalline structure of the SiC substrate* rather than to that of the SiC PECVD cladding.

No SiC diffraction peaks were also observed in XRD scans with SiC chips provided by CeTeV (see Sect. 4), without substrates. This was already observed a previous SiC sample analyzed at INAF/OAB [RD1]. The absence of Silicon Carbide XRD peaks for the cladding deposited by PECVD can be considered an evidence for either

1) an *amorphous structure* or

2) *monocristallinity* (with unknown orientation of the crystalline planes with respect to the surface)

of the sample. However, we shall see in the next section that the hypothesis 2) can be ruled out by further XRD investigations. Moreover, the very low density of the material (50% of the crystalline SiC density, see Sect. 3.1) is another evidence in favor of the amorphous structure of these SiC cladding. Amorphous structure was also reported in literature [RD2] with SiC films deposited by DC Magnetron Sputtering.

4. Powder XRD and Cathodoluminescence (CL) measurements at CNR-IMEM

Further XRD and CL measurements (performed at ***CNR-IMEM***, Parma) *confirm the amorphous structure of SiC chips* deposited with the current deposition system.

a) *No diffraction peaks were observed* also with the X-ray facility at CNR-IMEM (see Sect. 3.3), *even by checking all the possible orientations of crystalline planes* with respect to the incident X-ray beam.

b) by means of ***XRD measurements*** performed on powder obtained by milling some SiC chips, *no diffraction peaks were detected*. This result is extremely significant because it rules out the hypothesis of monocrystallinity: if the sample were a single crystal, diffraction peaks would be seen in powder diffraction as all preferred orientations would be lost.

b) performing ***Cathodoluminescence measurements*** (i.e. the analysis of the light emission caused by the excitation of the material by an electronic beam in a SEM), a typical broad emission spectrum due to de-excitation from the conduction to the valence band should be observed in presence of a crystalline structure. Indeed (see Fig. 12, red line), the CL spectrum of SiC samples is flat, especially when compared with the CL spectrum (blue plot, a broad peak around 550 nm) of a crystalline SiC epitaxial layer grown at CNR-IMEM.

CNR-IMEM

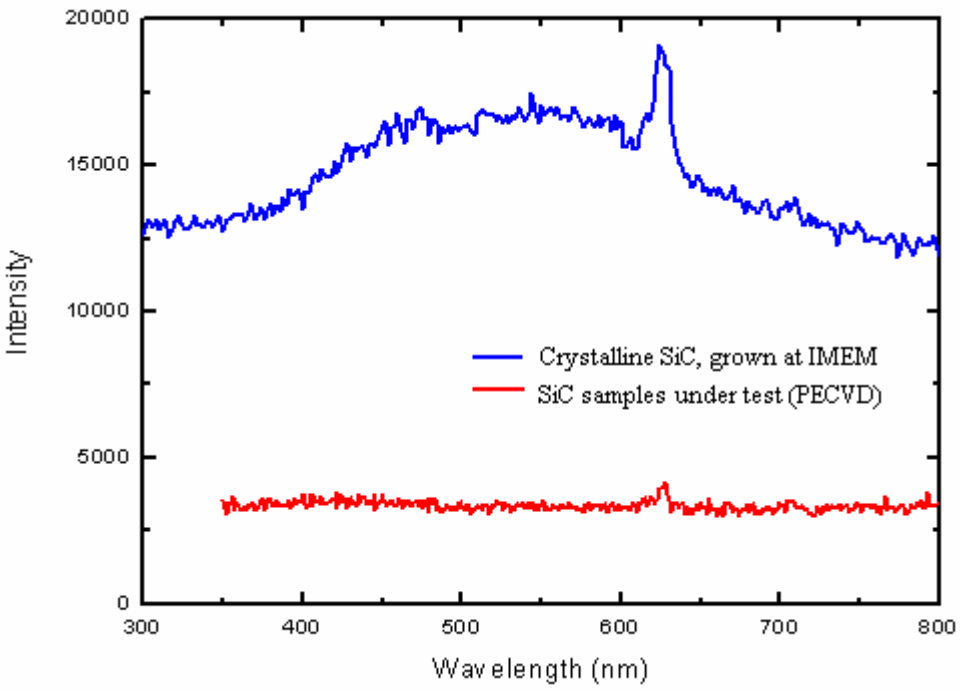

Fig. 12: a CL spectrum of the SiC samples chips under test (red line) compared with the CL emission spectrum from a SiC sample deposited at CNR-IMEM (courtesy by CNR-IMEM, *Parma, italy)*

5. SEM measurements

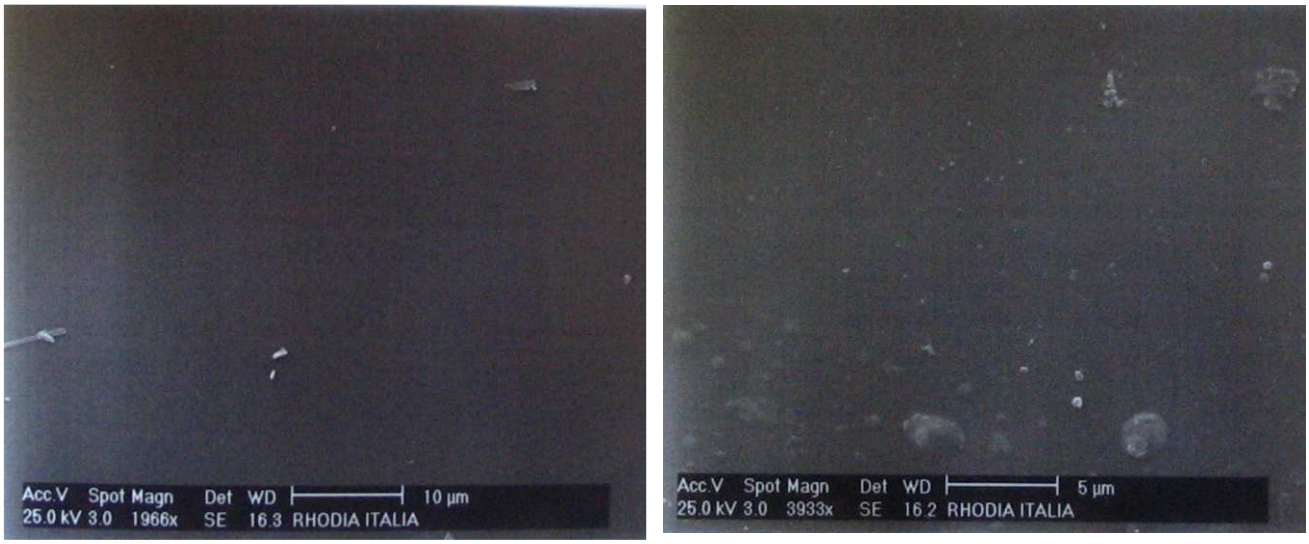

Fig. 13:SEM images of the surface of a PECVD SiC chip. (left) a major surface extent does not exhibit apparent surface features on 10 µm scales. (right) a minor surface extent is covered by small defects in ejection (courtesy by Rhodia Italia, *Ceriano Laghetto, Italy).*

SEM measurements were also performed on PECVD SiC samples: for technical reasons, the analysis was carried out on SiC chips provided by CeTeV. Some images *(kind courtesy by* Rhodia Italia, *Ceriano Laghetto, Italy)* are shown in Fig. 13: the surface appears quite smooth and isotropic almost everywhere (some micron wide defects are visible, but they cover a small percent of the surface).

In addition, we show in Fig. 14 the X-ray spectrum generated during the SEM measurements. The emission X-ray lines are a clear signature of the chemical elements present in the sample: the Kα X-ray lines of Silicon, Carbon and Oxygen are clearly detected. Note that the heights of the peaks are NOT proportional to the relative abundance of the elements in the sample.

In addition to the obviously expected lines of Si and C, only Oxygen is present in the analyzed sample. Other contaminants were not detected. The presence of the Oxygen could be due to a thin oxide layer at the samples surface [RD2]. The oxide layer did not cause apparent interference fringes in the XRR measurements, therefore its thickness should be limited to a few nanometers.

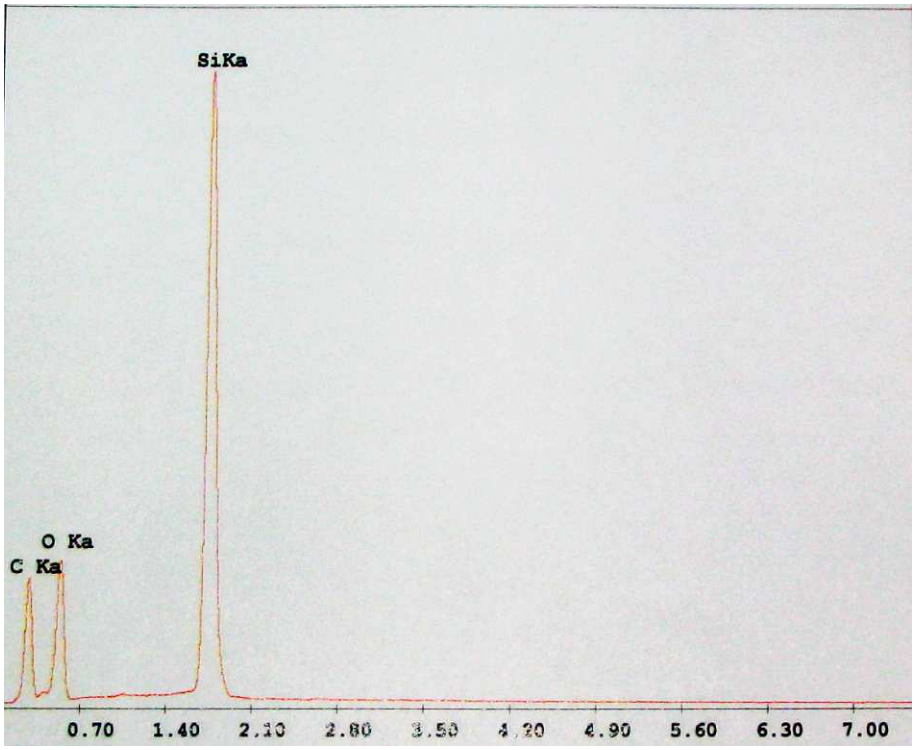

Fig. 14: The X-ray emission spectrum of a PECVD SiC chip, as measured during the SEM measurements of Fig. 10 (courtesy by Rhodia Italia, *Ceriano Laghetto, Italy). The vertical scale is linear (arbitrary units). The height of the peaks is not proportional to the relative abundances of the elements.*

6. Visible - NIR light reflectance measurements

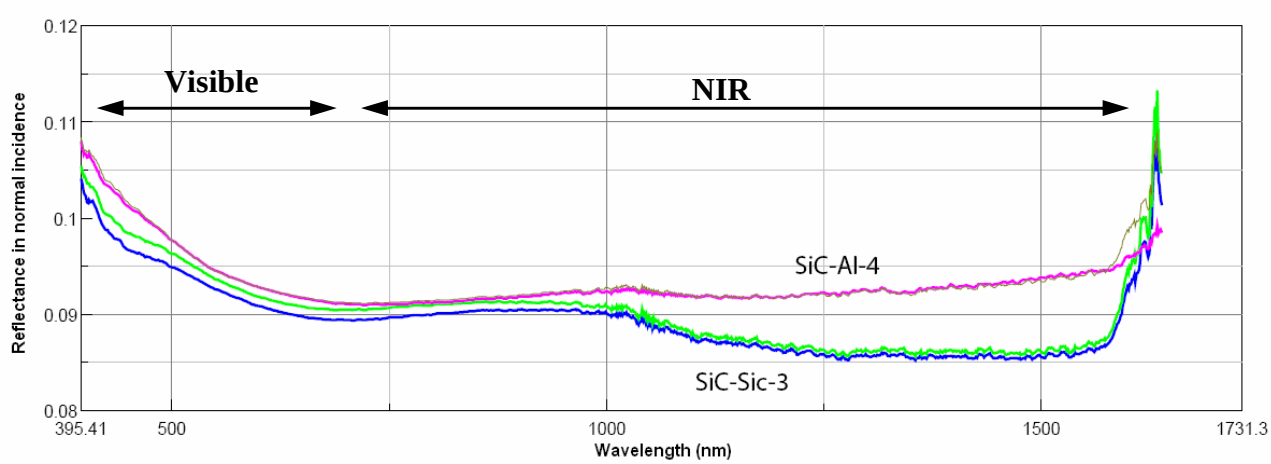

Fig. 15: the reflectance of two samples in normal incidence from 400 to 1700 Å photon wavelength, measured with the FILMETRICS spectrometer at Politecnico di Milano (measurement and image by G. Toso*).The curves appear doubled because the measurement has been repeated to ensure the repeatability of the results. The vertical scale is very stretched.*

The reflectivity of some samples has also been measured in visible light and NIR (Near Infrared) using the FILMETRICS spectrometer operated at *Politecnico di Milano*. The reflectivity of two samples (a SiC-SiC and a SiC-Al) in normal incidence from 400 up to 1700 nm photon wavelength is plotted in Fig. 15.

The reflectance of both samples appears similar but in the infrared band, where the reflectivity of the SiC-SiC is slightly lower. The average reflectivity is 9-10% vs. 20% expected from a modelization using the optical constants of *crystalline* SiC. The microroughness (6-7 Å, even at the lowest spatial frequencies) is too low, when compared to λ, to cause a so large decrease of the reflectivity, thus the discrepancy should be searched in the amorphous structure of the SiC cladding (Sect. 3.3).

We have no optical constants at our disposal for amorphous SiC at these wavelengths, hence we cannot deal with a detailed comparison. However, using the measured reflectivity (R ~ 0.1) we can derive from the Fresnel formula in normal incidence a refractive index $\mathbf{n_a \approx 1.97}$, without considering the photoabsorption. The average refractive index of crystalline SiC is $\mathbf{n_c \approx 2.8}$, much higher then the measured one.

The lower refractive index can be justified on the basis of the lower material density, as *n-1* is usually proportional to the material's polarizability, which is in turn proportional to its density. In our case, the ratio $(n_a\text{-}1)/(n_c\text{-}1) \approx \mathbf{0.5}$, the same value of the measured/crystalline ***density*** values ratio.

7. VUV reflectance measurements

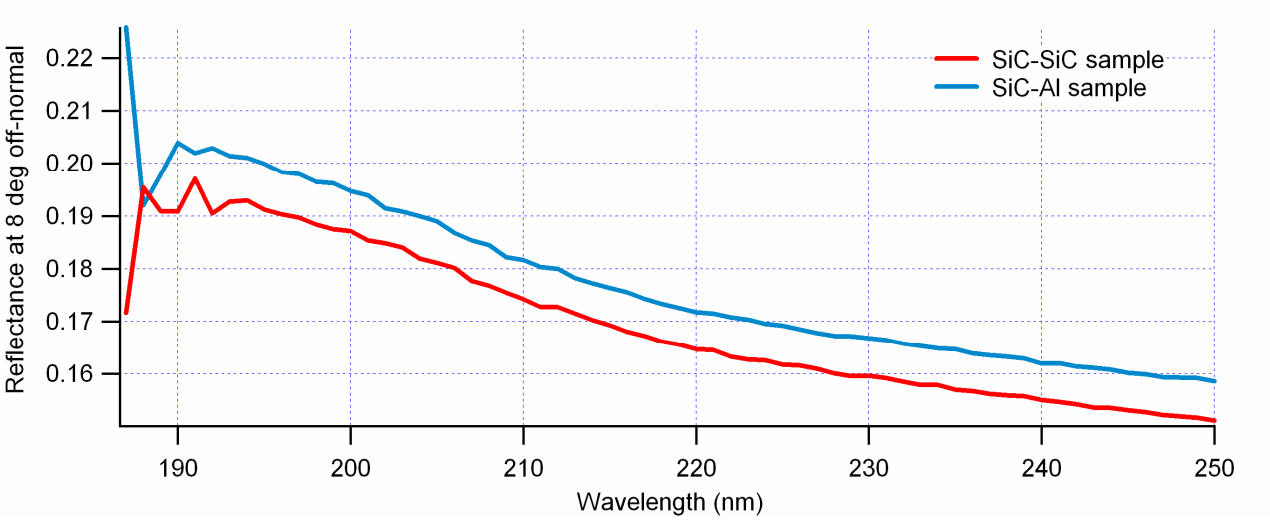

Fig. 16: the measured reflectance, at 8 deg off-normal, of a SiC-SiC sample and a SiC-Al sample in the VUV light (from 180 to 250 nm wavelength, measured at LUXOR-INFM, Padova, Italy, *courtesy by* P. Nicolosi).

The samples reflectance in the VUV light has also been measured at LUXOR-INFM (Padova, Italy), from 180 to 250 nm wavelength, at a 8 deg off-normal incidence angle.

Even if also in this wavelength range we have no optical constants for amorphous SiC, we can observe that the reflectivity is approximately halved with respect to the reflectance of crystalline SiC. Such a reduction is hardly explained by surface roughness, since the surface rms would have to be $\sigma \sim 16.5$ nm. A more realistic hypothesis is (as mentioned in the Sect. 6) the reduction of reflectivity due to a much smaller refractive index caused by the much smaller density (1.5 g/cm³ , see Sect. 3.1) with respect to the bulk density value of SiC (3.2 g/cm³).

The surface roughness could be, instead, responsible for the different reflectance of the two samples, even though this difference is only 5% of the SiC-Al reflectance: the smallness of the difference of the two samples classes is due to the large wavelength in use when compared with the actual roughness values of the surface (see Tab. 1).